Power Optimization of Nonlinear QAM Systems with Data Predistortion

Li-Chung Chang
Department of Electrical Engineering
National Taiwan University of Science and Technology
Taipei 106, TAIWAN

James V. Krogmeier
School of Electrical and Computer Engineering
Purdue University
West Lafayette, IN 47907-1285, USA

***Abstract*— In this paper, the data predistorter with memory used to minimize total power consumption due to amplifier nonlinearity in single power mode quadrature amplitude modulation(QAM) systems is investigated. The design of the data predistorter (DP) with memory is independent of the operating optimality criterion but depends upon the operating point of amplifier nonlinearity. The more useful choice of the operating optimality criterion which determines the optimum operating point of the amplifier is based on the DC power characteristic of the amplifier.**

I. Introduction

In the literature, predistortion techniques can be classified into two categories: signal predistorters [1], [2] and data predistorters [3], [4]. To eliminate the amplifier nonlinearity and linearize the channel, a signal predistorter (SP) implemented by either analog circuits or digital baseband components nonlinearly modifies the shape of the transmitted signal pulse. On the other hand, a data predistorter (DP) implemented by digital baseband components nonlinearly modifies the values of the transmitted data symbols, which then linearly modulate the pulse shape before the overall signal is nonlinearly amplified.

In a nonlinear channel with shorter memory, a memoryless DP provides competitive performance compared to a SP [5]. In a nonlinear channel with longer memory, a DP with memory can compensate the performance loss of a memoryless DP related to a SP [4]. A DP operating at the symbol rate does not cause spectral regrowth (in the sense that if pulse shaping is bandlimited, a DP preceding the pulse shaping filter will not change the bandwidth, although it will shape the spectrum). In addition, a DP is likely to have an advantage in the complexity issue in single carrier QAM systems. In conventional satellite communication systems, it is desirable to fully utilize the power capability of the on-board power amplifier, namely, to operate the power amplifier near its maximum output power. Such systems typically operating at a fixed output power level are here referred to as "single power mode" systems.

In order to quantify performance when nonlinearity and power-conversion efficiency are considered, different objective functions have been introduced in the literature. We have shown that minimizing total bit energy-to-noise power density ratio (E_t/N_0) is minimizing total power for a target BER. Furthermore, both E_t/N_0 and total degradation (TD) result in identical design for fixed DC bias power amplifiers with constant DC power [6]. To minimize total power consumption due to amplifier nonlinearity, the focus of this paper is to further investigate the digital baseband data predistortion technique in [4] to find the optimum operating point of the power amplifier in single power mode QAM systems. The organization of three types of the data predistorter with memory is introduced. The ideas to design and implement such data predistorters are demonstrated. In terms of the above two objective functions and two amplifier models, we present simulation results to demonstrate that the data predistorter with memory is an effective technique.

This paper is organized as follows. In Section II, we describe the system model, including the amplifier model and the QAM system. In Section III, we introduce three types of the data predistorter with memory. In Section IV, we present simulation results. Finally, Section V concludes the paper.

II. System Model

The block diagram of the baseband-equivalent QAM system with predistortion, which is used for simulations in this chapter, is shown in Fig. 1. The symbol sequence $\{a_n\}$ is an independent and identically distributed T-spaced sequence of complex symbols chosen from a square 16-QAM constellation with equal probabilities. The output of the data predistorter is denoted by the sequence $\{b_n\}$. Root raised cosine filters with roll-off factors of 0.25 are used in the transmitter and receiver (both truncated to a length of 16 symbols). The cascade of the transmit and receive filters produces a raised cosine filter with a unit voltage gain at the center. The relative (normalized) saturation input and output voltages of the amplifier model are both set equal to 1. Two types of nonlinear amplifier models are considered: the traveling wave tube amplifier (TWTA) and the solid state power amplifier (SSPA). In either case, the output $y(t)$ of the nonlinear amplifier is given by

$$y(t) = \mathcal{F}\left(|x(t)|\right) \exp\left(j\Phi(|x(t)|) + j \arg\left(x(t)\right)\right) \qquad (1)$$

where $|x(t)|$ is the amplitude (nonnegative voltage envelope) of $x(t)$, $\arg\left(x(t)\right)$ is the phase of $x(t)$, $\mathcal{F}(\cdot)$ is the AM/AM conversion and $\Phi(\cdot)$ is the AM/PM conversion. The AM/AM of the TWTA is a Saleh's model whereas that of the SSPA is a model proposed in [7].

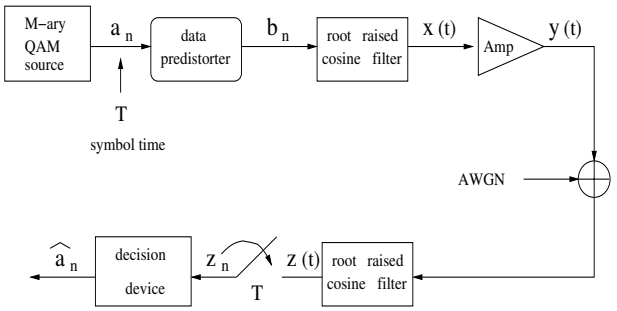

Fig. 1. Predistorted baseband QAM system model.

For the TWTA

$$\begin{aligned} \mathcal{F}(A) &= \frac{2A}{(1+A^2)} \\ \Phi(A) &= \frac{\pi}{3}\frac{A^2}{(1+A^2)}, \end{aligned} \tag{2}$$

and for the SSPA

$$\begin{aligned} \mathcal{F}(A) &= \frac{2A}{\left[1+(2A)^6\right]^{1/6}} \\ \Phi(A) &= 0 \end{aligned} \tag{3}$$

where $A = |x(t)|$. Compared to (2), the AM/AM of the SSPA model in (3) is chosen to obtain a normalized characteristic with the same small signal power gain of 6 dB and slightly better linearity in the low power region. The output backoff (OBO) which describes the output power level $P_o = \mathcal{F}^2(A)$ is defined as

$$OBO = P_{sat}/\overline{P_o} \tag{4}$$

where P_{sat} is the saturation (maximum) output power of the amplifier and the overbar indicates the mean resulting from a time-average. The output $y(t)$ is then disturbed by an additive white Gaussian noise (AWGN) and filtered by the root raised cosine filter and sampled per symbol time interval assuming perfect carrier and symbol synchronization. The sampled output of the receiver filter corresponding to the desired symbol a_n is denoted by z_n (in simulations a time delay is incorporated so that this correspondence holds). The decision device applies a set of thresholds to produce an estimate $\widehat{a_n}$ of a_n. The two resulting sequences are compared to calculate the symbol error rate (SER). Assuming that Gray code is employed, the BER is obtained by dividing the symbol error rate by $\log_2 M$ (strictly speaking this relationship between SER and BER holds only forv relatively low SER).

III. Data Predistorter with Memory

A trend in current communication systems is to employ baseband pulse shaping via digital signal processing before sending the signal through a power amplifier. This results in a nonlinear channel with memory. It was shown in [4] that adding memory to the data predistortion results in a significant performance improvement over memoryless data predistortion when the nonlinear channel has memory.

TABLE I

Formulas to compute the corresponding index number

DP type	the corresponding index number
(S_{n-1}, a_n, S_{n+1})	$I_n + g(I_{n+1})M + g(I_{n-1})M(M/4)$
(a_{n-1}, a_n, a_{n+1})	$I_n + I_{n+1}M + I_{n-1}M^2$
$(S_{n-2}, a_{n-1}, a_n, a_{n+1}, S_{n+2})$	$I_n + g(I_{n+2})M + I_{n+1}M(M/4) + I_{n-1}M^2(M/4) + g(I_{n-2})M^3(M/4)$

The DP with memory in [4] is based on global compensation of the nonlinearity. Each predistorted symbol b_n is a function of past, present, and future input symbols (a_{n-L}, $\cdots$,a_{n-1},a_n,a_{n+1} $\cdots$, a_{n+L}) where $2L+1$ is the memory length. Consider an $M-$point desired signal constellation. Memoryless DP has a look-up table with M entries only, whereas the DP with memory has a look-up table with M^{2L+1} entries (M^{2L} predistorted values for each symbol in the $M-$point signal constellation). As a result, the DP with memory can be expected to further reduce the nonlinear ISI and outperform memoryless DP.

A. The Organization of the Look-up Table

The DP with memory can be implemented via a look-up table structure. One potential problem of the DP with memory is that the required number of memory entries in the look-up table may be very large for some M and L. In order to reduce the required number of memory entries, the set-partitioning concept in which the signal constellation is partitioned into a number of square subsets composed of adjacent points in the same quadrant is developed. In the following, S_n denotes the subset of 4 points which includes a_n. Fig. 2 shows a 16-QAM constellation with such a grouping scheme. By considering S_n instead of a_n, the required number of memory entries can be divided by a factor of four at the expense of performance degradation.

A systematic way to access a specific entry in the look-up table is necessary in the programming design. One approach is to assume the index number (an integer) of the first entry is zero. For M-QAM, label the M states taken by a_n with integers from 0 to $M-1$. Let I_n denote the corresponding integer for a_n. Similarly, label the $M/4$ states taken by S_n with integers from 0 to $M/4-1$, and let $g(I_n)$ denote the corresponding integer for the subset to which a_n belongs. Table I shows the formulas to compute the corresponding index number of the memory entry in the look-up table for three types of the DP with memory. The formula used for (S_{n-1}, a_n, S_{n+1})-type DP is explained in Fig. 3. The other two formulas can be derived in similar ways.

B. Design and Implementation

The target signal constellation in the design of the DP with memory is selected to be a square M-QAM signal constellation in the absence of AWGN. The objective of the DP with memory is to find the optimum predistorted symbol in each look-up table entry in order to achieve the following

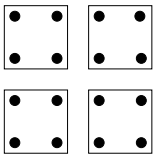

Fig. 2. Grouping of 16-QAM.

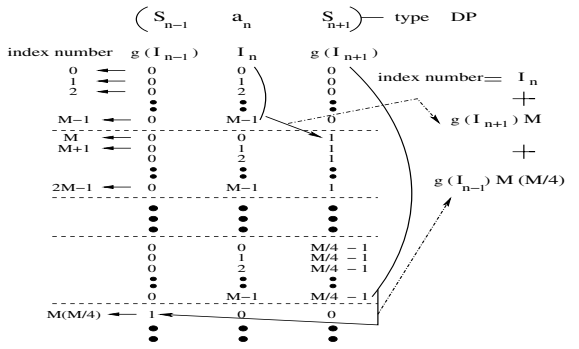

Fig. 3. Explanation of computing the index number for (S_{n-1}, a_n, S_{n+1})-type DP.

overall amplitude and phase responses between a_n and z_n in Fig. 1:

$$\begin{aligned} R_n &= \begin{cases} \rho_n, & \rho_n \le 1 \\ 1, & \rho_n > 1 \end{cases} \\ \Psi_n &= \phi_n \end{aligned} \tag{5}$$

where $R_n = |z_n|$, $\Psi_n = \arg(z_n)$, $\rho_n = |a_n|$ and $\phi_n = \arg(a_n)$, i.e., $z_n = a_n$ up to the saturation point where the relative input power is 0 dB. After the saturation point, z_n has the same phase as a_n but its amplitude is fixed to one because the peak amplitude constraint is set to be one.

It is important to note that, for an ideal model (also a pretty good assumption in practice), the DC bias scheme of the amplifier in a certain Class operation does not affect amplifier nonlinearity but is related to the degree of amplifier efficiency [8]. As a result, the DC bias scheme of the operating amplifier has no effect on finding the optimum look-up table at each OBO. However, it does have an effect on determining the look-up table corresponding to the optimum operating point in single power mode systems since the optimum operating point represents the best tradeoff between amplifier nonlinearity and efficiency.

An off-line iterative procedure can be used to achieve (5) in a least squares sense [3]. Let b_j be the predistorted point in the j-th look-up table entry, a_j be the corresponding input symbol to be predistorted and z_j be the corresponding output point after the receiver filter, $j = 1, 2, \cdots, N$ where N is the total required number of memory entries in the look-up table. At the k-th iteration to update b_j, the following iterative procedure is used:

$$\begin{aligned} r_j(k+1) &= \begin{cases} r_j(k) - \alpha e_j^r(k), & \rho_j \le 1 \\ 1, & \rho_j > 1 \end{cases} \\ \theta_j(k+1) &= \theta_j(k) - \alpha e_j^\theta(k) \end{aligned} \tag{6}$$

where $r_j(k) = |b_j(k)|$, $\theta_j(k) = \arg(b_j(k))$, α is a step-size parameter, and $e_j^r(k)$, $e_j^\theta(k)$ are the measured amplitude and phase errors for b_j at the k-th iteration, i.e., $e_j^r(k) = |\mathrm{E}\{z_j\}(k)| - |a_j|$ and $e_j^\theta(k) = \arg(\mathrm{E}\{z_j\}(k)) - \arg(a_j)$. The notation $\mathrm{E}\{z_j\}(k)$, obtained from a direct averaging of a number of output symbols z_j generated from the $k-1$-th to the k-th iteration, represents an estimate of the center of gravity of the corresponding subcluster at the receiver output. It is used to update b_j to reduce adaptation noise instead of updating b_j on a symbol-by-symbol basis [4].

Notice that from (5), for a given input signal constellation ($\{a_j\}$), the above iterative procedure can be used to find the corresponding optimum predistorted symbols in this look-up table with N memory entries. The term "optimum look-up table" will be used as the abbreviation of "optimum predistorted symbols in a look-up table with N memory entries" in the sequel. For a new input power level of $\{a_j\}$ which also represents the new reference signal constellation at the decision device in Fig. 1, a corresponding optimum look-up table has to be found by using the same iterative procedure. As a result, there is a one-to-one relationship between optimum look-up tables and power levels of $\{a_j\}$ in Fig. 1. For single power mode systems, the optimum operating point of the amplifier can be found to be the OBO which minimizes total degradation (TD) for those amplifiers with fixed DC power consumption such as fixed DC bias Class A amplifiers. For amplifiers with adaptive DC power consumption such as fixed or adaptive DC bias controlled Class A, Class AB and Class B amplifiers, E_t/N_0 is a better objective function to find the optimum operating point of the amplifier. Once the optimum OBO has been determined, the optimum look-up table corresponding to the optimum OBO is adopted for the system operation.

IV. Simulation Results

Monte-Carlo simulations using Matlab were performed with 4 samples per symbol. At least $10/(\text{target BER})$ symbols were generated to estimate the BER.

TWTA Model

The simulation results are shown in Fig. 4 - Fig. 6 for each type of the DP with memory. The TDs for three targets BERs (10^{-3}, 10^{-4} and 10^{-5}) are shown indicating how TD varies with both OBO and the target BER. At each OBO, TD increases as the target BER decreases. Notice that the optimum OBO which minimizes TD is a function of the target BER. The trend is that the lower the target BER, the higher the optimum OBO. This is reasonable since more backoff is necessary to reduce nonlinearity in order to reach lower BER. In terms of the value of the minimum TD for each DP, the degradation differences in TD tend to increase as the target BER decreases. More specifically, the increase in the value of minimum TD as the target BER gets lower is most significant for (S_{n-1}, a_n, S_{n+1})-type DP and least significant for $(S_{n-2}, a_{n-1}, a_n, a_{n+1}, S_{n+2})$-type DP. This shows adding memory improves robustness

of the DP to variation in the target BER. Based on the results in Fig. 4 - Fig. 6, a general conclusion in terms of TD for each OBO is that $(S_{n-2}, a_{n-1}, a_n, a_{n+1}, S_{n+2})$-type DP outperforms (a_{n-1}, a_n, a_{n+1})-type DP which outperforms (S_{n-1}, a_n, S_{n+1})-type DP at each target BER as expected. For each target BER, the optimum OBO of (S_{n-1}, a_n, S_{n+1})-type DP is the highest and that of $(S_{n-2}, a_{n-1}, a_n, a_{n+1}, S_{n+2})$-type DP is the lowest, which indicates that $(S_{n-2}, a_{n-1}, a_n, a_{n+1}, S_{n+2})$-type DP can be used to get more output power out of the power amplifier.

SSPA Model

For the SSPA model in (3), it has been observed that $OBO \leq 6$ dB is the power range that needs to be considered (3 dB smaller than the power range to be considered for the TWTA model). This result is mainly due to the fact that the SSPA model has zero AM/PM.

The simulation results are shown in Fig. 7 - Fig. 9 for each type of the DP with memory. All the above observations found in the TWTA model also apply to the SSPA model. All three types of the DP with memory result in better performance for the SSPA model compared to the TWTA model as expected. Compared to the TWTA model, the performance differences between $(S_{n-2}, a_{n-1}, a_n, a_{n+1}, S_{n+2})$-type DP, (a_{n-1}, a_n, a_{n+1})-type DP and (S_{n-1}, a_n, S_{n+1})-type DP at each target BER is smaller.

To illustrate the use of E_t/N_0 for amplifiers with adaptive DC power consumption, the amplifier circuit model called **sample_PA** (a Motorola MOSFET SSPA) in Agilent's advanced design system (ADS) software is simulated at a carrier frequency 800 MHz. Fig. 10 shows the results from both actual circuit simulation and the AM/AM of the SSPA model in (3), where relative input power $= 0$ dB is 199.5 mW and relative power $= 0$ dB is 1328.5 mW. The AM/AM of the SSPA model is a fairly good approximation. Therefore, the adaptive DC power characteristic generated from the circuit simulation presents a reasonable model for the SSPA model in (3), and it is employed in the simulations. Fig. 11 shows one of the simulation results based on (3) and the DC power characteristic in Fig. 10. From the results in Fig. 8 and Fig. 11, the resulting optimum OBOs which minimize E_t/N_0 are further backed off around 0.5 dB.

V. Conclusions

Three types of the DP with memory have been used to investigate the performance in single power mode QAM systems in terms of TD and E_t/N_0. The optimum operating point of the amplifier determines the optimum look-up table to be employed. The effectiveness of the DP with memory has been shown for both the TWTA and SSPA model.

References

[1] A. N. D'Andrea, V. Lottici, and R. Reggiannini, "RF power amplifier linearization through amplitude and phase predistortion," *IEEE Transactions on Communications*, vol. 44, no. 11, pp. 1477–1484, November 1996.

[2] J. K. Cavers, "Amplifier linearization using a digital predistorter with fast adaptation and low memory requirements," *IEEE Transactions on Vehicular Technology*, vol. 39, no. 4, pp. 374–382, November 1990.

[3] A. A. M. Saleh and J. Salz, "Adaptive linearization of power amplifiers in digital radio systems," *Bell Syst. Tech. J.*, vol. 62, no. 4, pp. 1019–1033, April 1983.

[4] G. Karam and H. Sari, "A data predistortion technique with memory for QAM radio systems," *IEEE Transactions on Communications*, vol. 39, no. 2, pp. 336–344, February 1991.

[5] G. Karam and H. Sari, "Analysis of predistortion, equalization, and ISI cancellation techniques in digital radio systems with nonlinear transmit amplifier," *IEEE Transactions on Communications*, vol. 37, no. 12, pp. 1245–1253, December 1989.

[6] L. Chang and J. Krogmeier, "Analysis of the effects of linearity and efficiency of amplifiers in QAM systems," *Proc. IEEE Wireless Communications and Networking Conference*, pp. 475–479, 2003.

[7] C. Rapp, "Effects of HPA-nonlinearity on a 4-DPSK/OFDM-signal for a digital sound broadcasting system," *Proceedings of the 2nd European Conference on Satellite Communications*, pp. 179–184, October 1991.

[8] K. Yang, G. Haddad, and J. East, "High-efficiency Class-A power amplifiers with a dual-bias-control scheme," *IEEE Transactions on Microwave Theory and Techniques*, vol. 47, no. 8, pp. 1426–1432, August 1999.

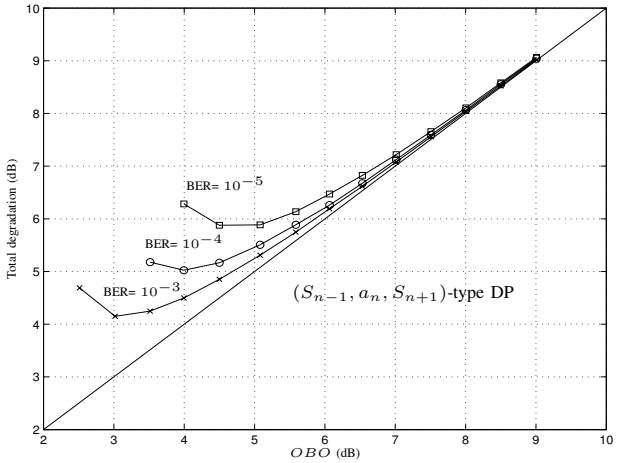

Fig. 4. Total degradation vs. OBO for 16-QAM and TWTA using (S_{n-1}, a_n, S_{n+1})-type DP.

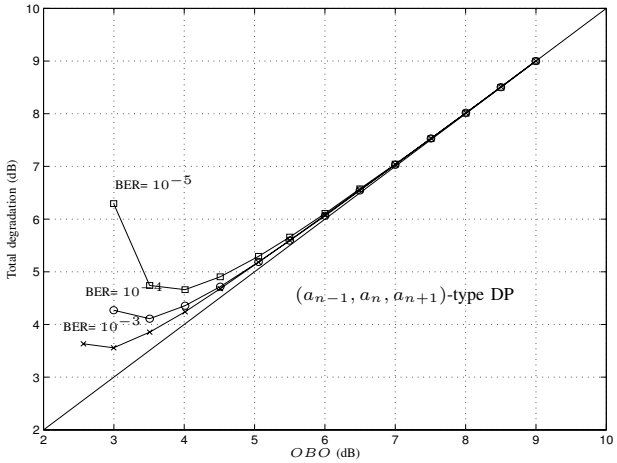

Fig. 5. Total degradation vs. OBO for 16-QAM and TWTA using (a_{n-1}, a_n, a_{n+1})-type DP.

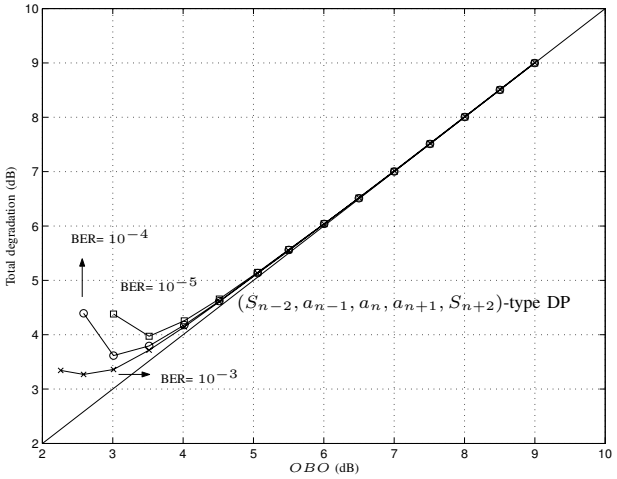

Fig. 6. Total degradation vs. OBO for 16-QAM and TWTA using $(S_{n-2}, a_{n-1}, a_n, a_{n+1}, S_{n+2})$-type DP.

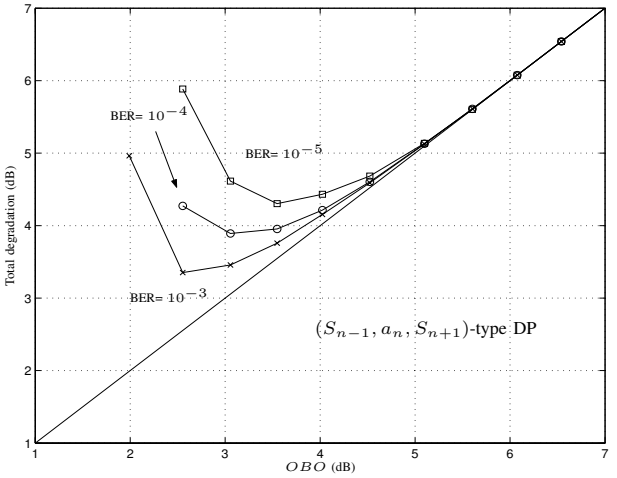

Fig. 7. Total degradation vs. OBO for 16-QAM and SSPA using (S_{n-1}, a_n, S_{n+1})-type DP.

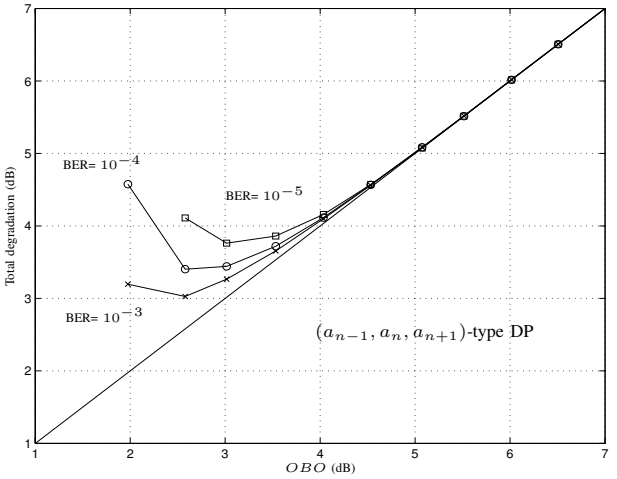

Fig. 8. Total degradation vs. OBO for 16-QAM and SSPA using (a_{n-1}, a_n, a_{n+1})-type DP.

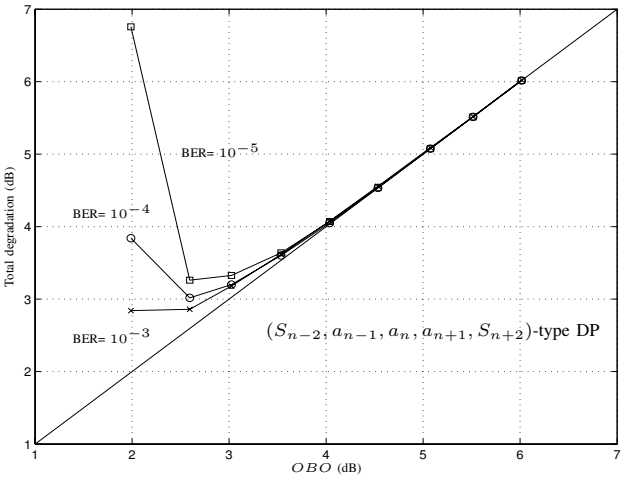

Fig. 9. Total degradation vs. OBO for 16-QAM and SSPA using $(S_{n-2}, a_{n-1}, a_n, a_{n+1}, S_{n+2})$-type DP.

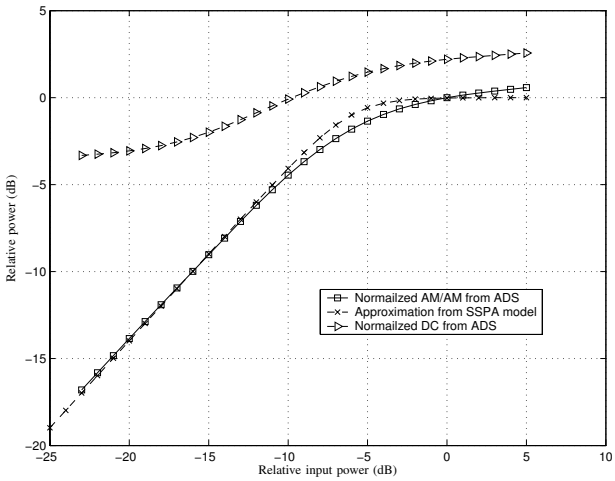

Fig. 10. AM/AM conversion and DC power from ADS circuit simulation tool.

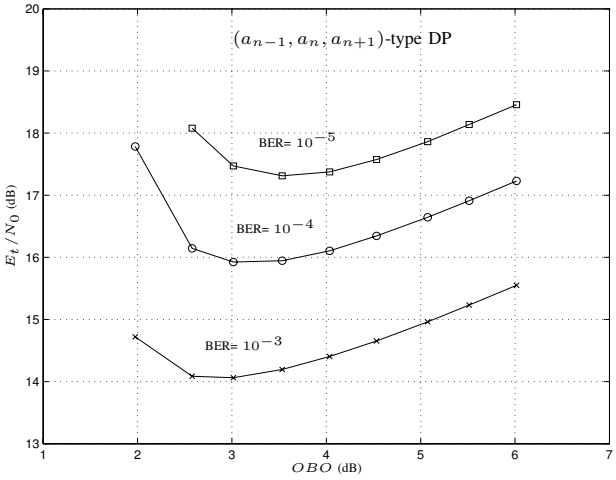

Fig. 11. E_t/N_0 vs. OBO for 16-QAM and SSPA with adaptive DC power using (a_{n-1}, a_n, a_{n+1})-type DP.